Journal of Theoretical and Applied Information Technology
30th April 2015. Vol.74 No.3

ISSN: 1992-8645 www.jatit.org E-ISSN: 1817-3195

MICROWAVE IMAGING FOR THE DETECTION AND LOCALIZATION OF BREAST CANCER USING ARTIFICIAL NEURAL NETWORK

[1]ABDELFETTAH MIRAOUI, [1, 2]LOTFI MERAD, SIDI [1]MOHAMED MERIAH

[1]University Abou Bekr Belkaid-Tlemcen, Faculty of Technology, Telecommunications Laboratory Tlemcen.

[2]Department of Physics, Preparatory School in Science and Technology, Bel-horizon, Tlemcen, Algeria

E-mail : af.miraoui@yahoo.fr , merad77@yahoo.fr , meriah_m@yahoo.com,

ABSTRACT

Localization and Reconstruction of homogenous objects from electromagnetic scattered fields have been shown to be of great importance, because of their various applications in many areas such as medicine, biology, geophysics and other sciences. In this paper, we propose a computational method for detection and localization of the object for medical application (breast cancer). The proposed technique is based on the use of artificial neural network ANN. A spherical tumor was created and at arbitrary locations in a breast model using an EM simulator. Bow-tie antennas were used to transmit and receive Ultra-Wide Band (UWB) signals at 4GHz. A training and validation sets were constructed to train and test the ANN. A very optimistic results have been observed for early received signal components with the ANN model. Hence, the proposed model is very potential for early tumor detection to save human lives in the future.

Keywords: *Microwave Imaging, Artificial Neural Network (ANN), Computer-Aided Diagnosis, Breast Cancer.*

1. INTRODUCTION

Breast cancer affects many women and early detection aids in fast and effective treatment. X-ray mammography is currently the most effective imaging method for detecting clinically occult breast cancer. However, despite significant progress in improving mammographic techniques for detecting and characterizing breast lesions, mammography reported high false-negative rates [1] and high false-positive rates [2].These difficulties are attributed to the intrinsic contrast between normal and malignant tissues at X-ray frequencies. For soft tissues like human breast, X-ray cannot image the breast anomalies at an early stage, as there is no significant variation in density between normal and malignant breast tissues [3].

Microwave imaging is a new technology that has potential applications in the field of diagnostic medicine [4, 5]. This expectation is based on the molecular interactions (dielectric) rather than atomic (density) based on microwave radiation with the target in comparison with X-ray imaging.

Many studies rely on microwave as a powerful electromagnetic tool to recover the physical and electrical properties of objects. For the application of detection and localization of breast cancer, microwave imaging has been very effective in the detection and localization of tumors at a very early stage.

The contrast between the dielectric properties of breast tissue creates multiple scattering of the wave in these tissues which presents a nonlinear inverse scattering problem. In this work, we use a novel technique based on neural networks, which was recently introduced in the detection and localization of objects by microwave imaging without solving this problem [5].

The proposed technique has been already used however, the database used is not enough large and the precision of localization is not better [6]. In our study, we have improved results by increasing the precision of detection and localization of tumors. For this, we used a larger database than that used in [6] with other learning algorithm. A spherical tumor was created and placed at arbitrary locations in a breast model using an EM simulator. Bow-tie antennas were used to transmit and receive Ultra-Wide Band (UWB) signals at 4GHz.

Journal of Theoretical and Applied Information Technology
30th April 2015. Vol.74 No.3

ISSN: 1992-8645 www.jatit.org E-ISSN: 1817-3195

The simulation results show that the ANN gives more precision in terms of detection and localization.

2. BREAST MODEL FOR DATA COLLECTION

In this paper, we have used a hemisphere shape model with the most common dimensions as presented in Figure 1 and Table 1 [6].

Table 1 : Model Parts Sizes

Model part	Size (cm)
Breast diameter	10
Breast height	6
Skin thickness	0.2
Chest thickness	2

The dielectric properties that have been used are shown in Table 2 where σ is the tissue conductivity in (Siemens/meter) and ε_r is the relative permittivity [7].

Table 2 : Dielectric Properties

	Conductivity σ (S/M)	Permittivity ε_r
Skin	1.49	37.9
Fat	0.14	5.14
Chest	1.85	53.5
Tumor	1.20	50

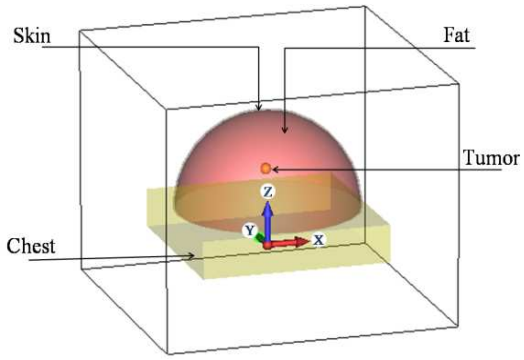

Figure 1: View Of The Model In CST

In the literature [8, 9] the tumor radius size ranges from 0.2 cm to about 1.5 cm or more, In this case, we took a tumor with a radius of 0.25 cm is close to its minimum size.

3. DETECTION AND LOCALIZATION A LONG ONE DIMENSION (1-D)

In this part, we propose a new stochastic approach based on artificial neural networks for detection and localization of the breast cancer. We will use a Scaled conjugate gradient « trainscg » as learning algorithm. A comparative study between the two algorithms (Gradient descent with momentum « traingdm » used in [6] and «trainscg») will be given in this paper.

3.1. CONSTRUCTION OF ARTIFICIAL NEURAL NETWORK

The construction of the neural network is done through an iterative process on samples of a previously built database [10]. This database contains a set of data (input / output) obtained by simulation using the software "CST" Figure 2. For this we proceeded as follows:

1. Place a pair of transmitter - receiver at opposite sides of breast model;
2. Place a tumor at any location in the model;
3. Transmit a Gaussian pulse of a plane wave in the direction of the x-axis;
4. Receive the signal on the opposite side;
5. Change tumor location and repeating the steps (3-4).

This process of data generation was performed for 45 different locations by moving the tumor along the axis 'y'. Also, breast model without tumor tissue was used 2 times to obtain signals propagated through the breast tissue. As a result, two groups of signals received were formed as follows:

- Group (1): a set of 38 signals (37 with tumor and 1 without tumors) were used for ANN learning;
- Group (2): a set of 9 signals (8 with tumor and 1 without tumors) were used for the test phase of the ANN;

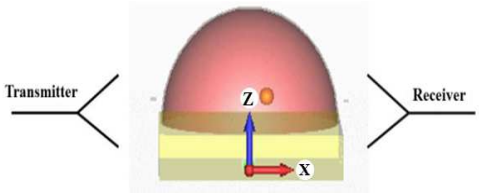

Figure 2 : Transmitter / Receiver System

3.2. PREPROCESSING DATA

The signals received by the receiver contain a number of samples that can be from 4500 to 7200 samples Figure 3.

To reduce the number of samples and to fix the sampling interval of the signal, we used a Cubic Hermite Interpolating Polynomial to generate a polynomial P (xi) while keeping the same pace of the signal [11, 12].The number of samples obtained

Journal of Theoretical and Applied Information Technology
30th April 2015. Vol.74 No.3

ISSN: 1992-8645 www.jatit.org E-ISSN: 1817-3195

after interpolation with a step of 0,01 in the segment (1,8 ns and 3,62 ns) is 183.

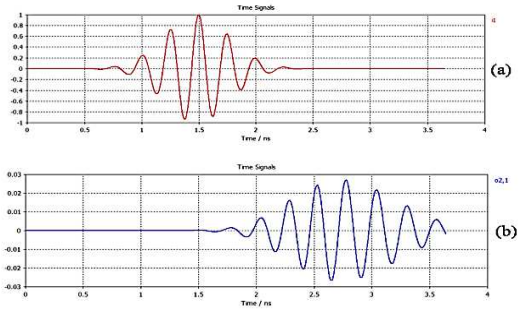

Figure 3: (A) Transmitted Signal, (B) Received Signal

There are no theoretical results, or even empirical rules that allow dimensioning a neural network based problem to resolve.

The design of a multilayer network is experimentally, the difficulty usually arises when choosing the number of hidden layer, and the number of the nodes in each hidden layer. After several tests, a multilayer network was selected with the topology presented in Figure 4.

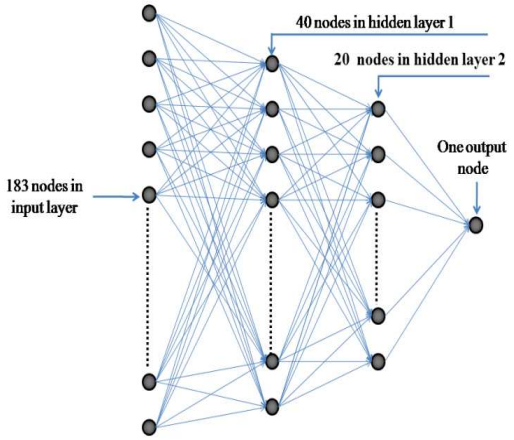

Figure 4: ANN Model For 1-D

3.3. LEARNING PHASE

When the network architecture has been agreed, the learning phase is used to calculate the synaptic points (Wi) for each node final. The used transfer function is "tansig" which has output in the range [−1, +1]. The parameters of the topology and training are summarized in Table 3.

Note that the values given in Table 4 are normalized values (relative to the diameter of the breast) because the output of the ANN can take values between -1 and 1; this is caused by the activation function (sigmoid).

Table 3: ANN Parameters In (1-D)

Parameters of ANN	Values
Training function	trainscg
Number of nodes in input layer	183
Number of nodes in hidden layer 1	40
Number of nodes in hidden layer 2	20
Number of nodes in output layer	1
Activation function	sigmoid
Number of iterations	500 000

When the learning phase is finished for the learning algorithm Figure 5, we tested the performance of ANN using group 2.

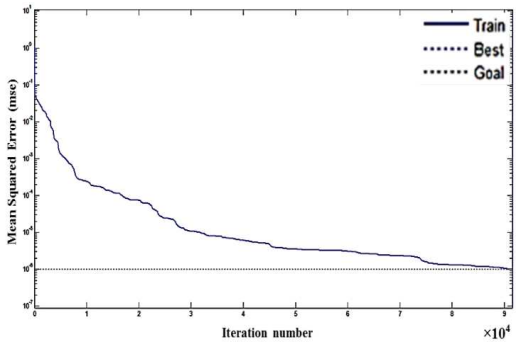

Figure 5 : Performance Learning Phase For Trainscg Algorithms (1-D)

Table 4 : Actual Tumor Position And Output Of ANN (1-D)

Actual tumor location (cm/10)	ANN output (cm/10) (SCG)
0,28	0.2919
0,4	0.3829
0,52	0.5641
0,6	0.5586
0,68	0.7039
0,78	0.7847
0,34	0.3041
0,46	0.4665
-1	-0.9998

The Table 4 shows that the learning algorithm "trainscg" gives better results. The outputs of ANN are very close to the real position imposed in the electromagnetic simulator (CST). The learning phase lasted 4 hours with an error of 10^{-6} Figure 5.

Journal of Theoretical and Applied Information Technology
30th April 2015. Vol.74 No.3

ISSN: 1992-8645 www.jatit.org E-ISSN: 1817-3195

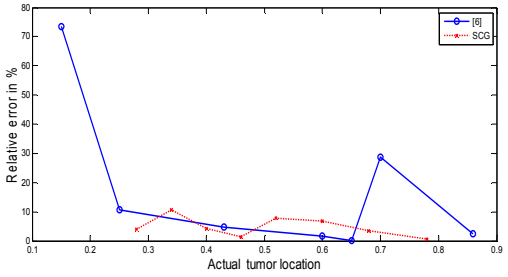

Figure 6: Performances Of ANN

Indeed, we gives in Figure 6, the performance of the ANN (SCG algorithm) by plotting the relative error versus the actual tumor location. As we can seen, the relative error obtained is less than obtained by [6].

4. DETECTION AND LOCALIZATION IN TWO DIMENSION (2-D)

For the detection and location of a tumor in two dimensions (2-D), we used the same simulation steps (1-D) given in paragraph 3.1. The procedure for data generation was performed for 481 different locations by displacing the tumor along the axes 'Y' and 'X'. Consequently, breast model without tumor tissue was used 2 times to obtain signals propagated through the breast tissue. Two groups of received signals were formed as follows:

- Group (1): a set of 432 signals (431 with tumor and 1 without tumors) were used for NN learning;
- Group (2): a set of 50 signals (49 with tumor and 1 without tumors) were used for the test phase of the ANN;

The parameters of the topology and learning are summarized in the Table 5 and Figure 7. The number of samples obtained after interpolation with a step of 0.01 in the segment (0,3 ns and 3 ns) is 271. The input layer, contains as many neurons as the number of elements of the input vector.

Table 5: ANN PARAMETERS In (2-D)

Parameters of ANN	Values
Training function	traingscg
Number of nodes in input layer	271
Number of nodes in hidden layer 1	40
Number of nodes in hidden layer 2	20
Number of nodes in hidden layer 3	12
Number of nodes in output layer	2
Activation function	sigmoid
Number of iterations	1 000 000

The same for the output layer contains as many neurons as the number of states to discriminate. Therefore, the input layer consists of 271 neurons and the output layer consists in to two neurons representing the position 'X' and 'Y' of the tumor in the breast model.

When the learning phase is finished Figure 8, we tested the performance of ANN using group 2.

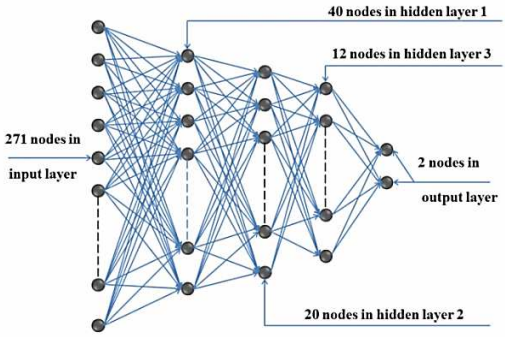

Figure 7: ANN Model For (2-D)

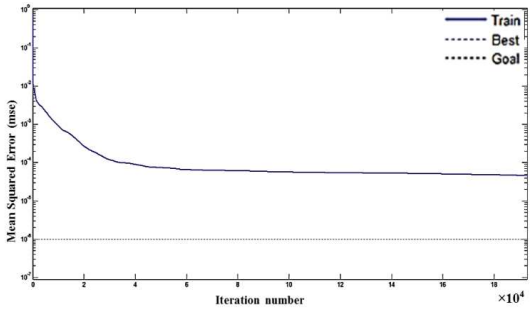

Figure 8 : Performance Learning Phase For Trainscg Algorithms (2-D)

Table 6 : Actual Tumor Position And Output Of ANN (2-D)

Actual tumor location(cm/10)		ANN output (cm/10)	
(X)	(Y)	(X)	(Y)
-1	-1	-0.9945	-1.0000
0.2600	0.4600	0.2552	0.4407
0.2800	0.5600	0.3193	0.5371
0.2800	0.4400	0.3428	0.4110
0.3000	0.5600	0.3095	0.5816
0.3000	0.4600	0.3008	0.4506
0.3200	0.5600	0.3107	0.5770
0.3200	0.4000	0.3309	0.4183
0.3400	0.5400	0.3465	0.5449
0.3400	0.4400	0.3383	0.4145

ISSN: 1992-8645 www.jatit.org E-ISSN: 1817-3195

0.3600	0.5400	0.3604	0.5360
0.3600	0.3800	0.3547	0.4007
0.3800	0.6400	0.3854	0.6358
0.3800	0.5400	0.4074	0.5412
0.3800	0.4600	0.4262	0.4618
0.4000	0.6400	0.4130	0.6371
0.4000	0.5400	0.3923	0.5076
0.4000	0.4200	0.3940	0.1523
0.4200	0.6000	0.4217	0.6016
0.4200	0.4600	0.4290	0.4619
0.4400	0.4600	0.4254	0.4682
0.4600	0.7200	0.4414	0.7716
0.4600	0.5600	0.4581	0.5499
0.4600	0.4000	0.4568	0.4128
0.4800	0.5800	0.4924	0.6462
0.4800	0.4400	0.4940	0.4398
0.5000	0.5600	0.4874	0.5369
0.5000	0.4200	0.4952	0.4543
0.5200	0.6000	0.5249	0.5677
0.5200	0.4600	0.5279	0.4685
0.5400	0.6200	0.5381	0.6773
0.5400	0.4000	0.5428	0.4128
0.5600	0.5400	0.5583	0.5353
0.5600	0.2800	0.5718	0.3673
0.5800	0.6600	0.5752	0.5814
0.5800	0.5600	0.5702	0.5482
0.5800	0.4000	0.5781	0.4054
0.6000	0.5400	0.5924	0.5068
0.6000	0.4200	0.5944	0.1808
0.6200	0.5800	0.6212	0.5587
0.6200	0.4400	0.6114	0.4238
0.6400	0.5400	0.6447	0.5288
0.6400	0.4400	0.6426	0.4348
0.6600	0.5800	0.6636	0.5823
0.6600	0.4400	0.6650	0.4431
0.6800	0.5400	0.6882	0.5339
0.6800	0.4000	0.6867	0.4185
0.7000	0.4600	0.7102	0.4595
0.7200	0.5400	0.7237	0.5372
0.7400	0.5400	0.7381	0.5439

The Table 6 shows the results of detection and localization in two dimensions where Scaled conjugate gradient algorithm is used for the learning phase. The learning phase lasted 11 hours with an error $2{,}35 \times 10^{-6}$.

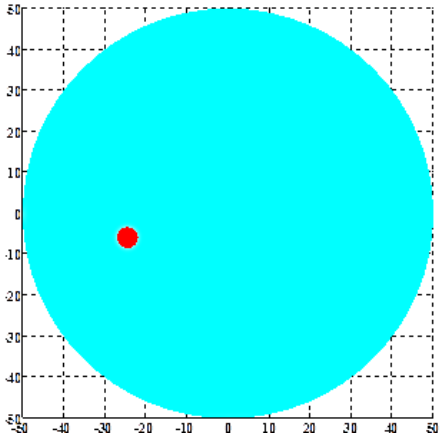

Figure 9 : Detection And Localization Of A Tumor At X=-22 Mm; Y=-6mm ($-50 \le X \le 50$ and $-50 \le Y \le 50$)

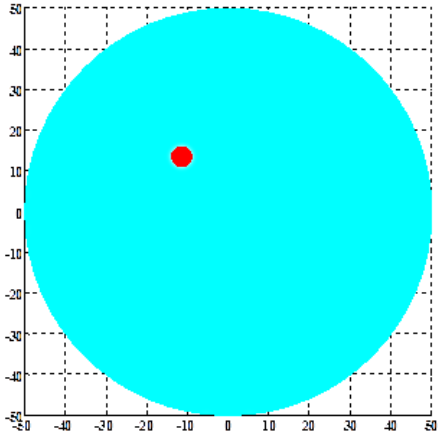

Figure 10 : Detection And Localization Of A Tumor At X=-10mm; Y=14mm ($-50 \le X \le 50$ and $-50 \le Y \le 50$)

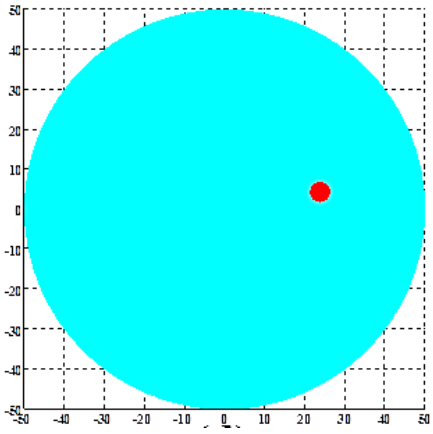

Figure 11 : Detection And Localization Of Tumor At X=22mm; Y=4mm ($-50 \le X \le 50$ and $-50 \le Y \le 50$)

Journal of Theoretical and Applied Information Technology
30th April 2015. Vol.74 No.3

ISSN: 1992-8645 www.jatit.org E-ISSN: 1817-3195

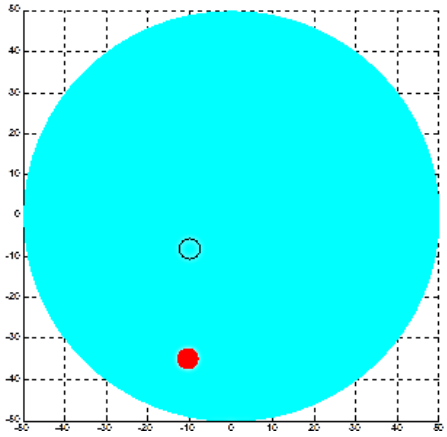

Figure 12 : Detection And Localization Of Tumor At X=-10mm; Y=-8mm ($-50 \le X \le 50$ and $-50 \le Y \le 50$)

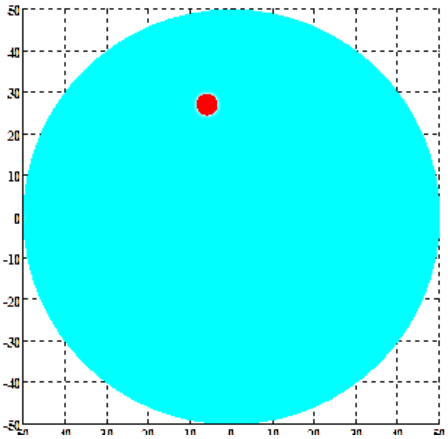

Figure 13 : Detection And Localization Of Tumor At X=-4mm; Y=-22mm ($-50 \le X \le 50$ and $-50 \le Y \le 50$)

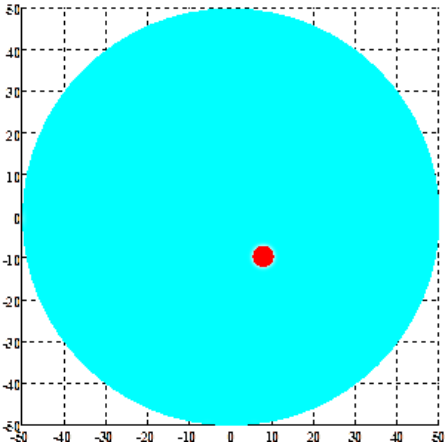

Figure 14 : Detection And Localization Of Tumor At X=10 Mm; Y=-8mm ($-50 \le X \le 50$ and $-50 \le Y \le 50$)

5. RESULTS

In the case of (1-D), we note that the positions obtained by the ANN of learning algorithm « traingscg » are very similar to real positions in 'CST' with a better detection rate which is in the order of 100% for the detection and localization Table 4.

Based on Table 6, we note that for input signals without the presence of a tumor, the output of ANN is negative and for input signals witch the presence of tumor, the output of ANN is positive this means that the detection rate is almost 100%. We also note, for input signals of ANN in the presence of a tumor at different positions, the output of ANN is very similar to the actual position in "CST", except for three cases where the output ANN is relatively far from there al position of the tumor in “CST” Table 6, where the localization rate is the range of 94%.

Figure 9, 10, 11, 12, 13 and 14 show examples of images for some signals of group (2). We show that for images (9), (10), (11), (13) and (14) the ANN output provides an position of tumor confused with real position of tumor in “CST”, which shows good tumor localization. However in the image (12), ANN output gives apposition far to there al tumor position of this latter in “CST”, where we have a wrong tumor localization.

6. CONCLUSION

In this work, a Artificial Neural Network was used for detection and localization the tumors in one and two dimensional based on the dielectric properties of human mammary tissues. The received signals were used to construct a database for the learning phase of ANN model. These simulation results are very satisfactory in terms of detection and localization.In future work we will study: detection and localization the tumors in three directions.

REFERENCES:

[1] J. G. Elmore, M. B. Barton, V. M. Moceri, S. Polk, P. J. Arena, and S. W. Fletcher “Ten year risk of false positive screening mammography and clinical breast examinations,” *New England Journal of Medicine,* Vol. 338, pp 1089–1096, 1998.

[2] E. C. Fear, S. C. Hagness, P. M. Meany, M. Okoniewski, and A. Stuchlym, “Enhancing breast tumor detection with near field

ISSN: 1992-8645 www.jatit.org E-ISSN: 1817-3195

imaging," *IEEE Microwave magazine,* Vol. 3, pp 48–56, 2002.

[3] E. C. Fear, X. Li, S. C. Hagness, and M. A. Stuchly, "Confocal microwave imaging for breast cancer detection: localization of tumors in three dimensions," *IEEE Transactions on Biomedical Engineering,* Vol. 49, pp 812–821, 2002.

[4] S. S. Chaudhary, R. K. A. Mishra, A. Swarup, and J. M. Thomas, "Dielectric properties of normal and malignant human breast tissues at radio wave and microwave frequencies," *Indian Journal of Biochemistry and Biophysics,* Vol. 21, pp 76–79, 1981.

[5] M. Lazebnik, and Al., "A large-scale study of the ultra-wideband microwave dielectric properties of normal, benign and malignant breast tissues obtained from cancer surgeries," *Phys. Med. Biol,* Vol. 52, 6093{6115, IOP Publishing, Oct. 2007.

[6] S. A. Alshehri, S. Khatum, and A. B. Jantan; "UWB imaging for breast cancer detection using neural network," *Progress In Electromagnetics Research C,* Vol. 7, pp 79–93, 2009.

[7] A. Miraoui, L. Merad, S. M. N. Meriah, Hassain, N. Benahmed, M. Bousahla, Taleb- A. Ahmed, and B. Belarbi, "Microwave Imaging for Breast Cancer Detection Using Artificial Neural Network," *International Congress on Telecommunication and Application, University of A.MIRA Bejaia, Algeria,* AM-P03, 2012.

[8] M. Miyakawa, T. Ishida, and M. Wantanabe, "Imaging capability of an early stage breast tumor by CP-MCT," *Proceedings of the 26th Annual International Conference of the IEEE EMBS,* Vol. 1, pp 1427–1430, San Francisco, CA, USA, 2004.

[9] E. C. Fear, and M. A. Stuchly, "Microwave detection of breast cancer," *IEEE Transactions on Microwave Theory and Techniques,* Vol. 48, pp 1854–1863, 2000.

[10] M. Wang, S. Yang, S. Wu, and F. Luo, "ARBFNN approach for DoA estimation of ultra-wideband antenna array," *Neurocomputing,* Vol. 71, pp 631–640, 2008.

[11] M. Miyakawa, T. Ishida, and M. Wantanabe, "Imaging capability of an early stage breast tumor by CP-MCT," *Proceedings of the 26th Annual International Conference of the IEEE EMBS,* Vol. 1, 1427–1430, San Francisco, CA, USA, 2004.

[12] S. Salmon "Analyse Numérique," *Université Louis Pasteur, L2 Mathématiques* 2005-2006.